fractal and fractional

MDPI

Article

Design and Application of an Interval Estimator for Nonlinear Discrete-Time SEIR Epidemic Models

Awais Khan [1,2,3], Xiaoshan Bai [1,3], Muhammad Ilyas [4], Arshad Rauf [5], Wei Xie [6], Peiguang Yan [2] and Bo Zhang [1,3,*]

1 College of Mechatronics and Control Engineering, Shenzhen University, Shenzhen 518060, China; awaiskhan@szu.edu.cn (A.K.); baixiaoshan@szu.edu.cn (X.B.)
2 College of Physics and Optoelectronic Engineering, Shenzhen University, Shenzhen 518060, China; yanpg@szu.edu.cn
3 Shenzhen City Joint Laboratory of Autonomous Unmanned Systems and Intelligent Manipulation, Shenzhen University, Shenzhen 518060, China
4 Department of Electrical Engineering, Balochistan University of Engineering and Technology Khuzdar, Khuzdar 89100, Pakistan; m.ilyas@buetk.edu.pk
5 College of Automation Engineering, Nanjing University of Aeronautics and Astronautics, Nanjing 210016, China; arshad@nuaa.edu.cn
6 College of Automation Science and Technology, South China University of Technology, Guangzhou 510641, China; weixie@scut.edu.cn
* Correspondence: zhangbo@szu.edu.cn

Abstract: This paper designs an interval estimator for a fourth-order nonlinear susceptible-exposed-infected-recovered (SEIR) model with disturbances using noisy counts of susceptible people provided by Public Health Services (PHS). Infectious diseases are considered the main cause of deaths among the top ten worldwide, as per the World Health Organization (WHO). Therefore, tracking and estimating the evolution of these diseases are important to make intervention strategies. We study a real case in which some uncertain variables such as model disturbances, uncertain input and output measurement noise are not exactly available but belong to an interval. Moreover, the uncertain transmission bound rate from the susceptible towards the exposed stage is not available for measurement. We designed an interval estimator using an observability matrix that generates a tight interval vector for the actual states of the SEIR model in a guaranteed way without computing the observer gain. As the developed approach is not dependent on observer gain, our method provides more freedom. The convergence of the width to a known value in finite time is investigated for the estimated state vector to prove the stability of the estimation error, significantly improving the accuracy for the proposed approach. Finally, simulation results demonstrate the satisfying performance of the proposed algorithm.

Keywords: interval analysis; interval estimator; finite-time convergence; bounded uncertainties; infectious diseases; SEIR epidemic model

Citation: Khan, A.; Bai, X.; Ilyas, M.; Rauf, A.; Xie, W.; Yan, P.; Zhang, B. Design and Application of an Interval Estimator for Nonlinear Discrete-Time SEIR Epidemic Models. *Fractal Fract.* **2022**, *6*, 213. https://doi.org/10.3390/fractalfract6040213

Academic Editors: Thach Ngoc Dinh, Shyam Kamal, Rajesh Kumar Pandey and Norbert Herencsar

Received: 24 January 2022
Accepted: 7 April 2022
Published: 9 April 2022

1. Introduction

There were around 30.2–45.1 million people living with HIV with 680,000 casualties in 2020, whereas an epidemic like seasonal influenza causes 3–5 million serious illness cases with 250,000–500,000 casualties each year worldwide according to the WHO [1,2]. The surveillance of infectious diseases plays a vital role in analyzing these epidemics, for instance, origin, spread and dynamics. PHS relies upon surveillance statistics collected by agencies such as the Chinese Center for Disease Control and Prevention (China CDC) for infected people to estimate the activity level of such diseases, intervention strategy preparation, and recommendations of design policies.

Mathematical modeling of epidemics plays a major role in organizing public health responses and developing early outbreak detection systems [3–7]. The first modern math-

ematical epidemic model, i.e., susceptible-infectious-recovered (SIR), was proposed by Kermack et al. in 1927 for cholera (London 1865) and plague epidemics (Bombay 1906, London 1665–1666) [8]. According to the SIR model, a fixed number of the population can be divided into three compartments at any time: susceptible individuals (not yet infected but can be infected in future), infectious individuals (those who have an infection and can infect others), and recovered individuals (who are recovered from the infection and are immune now). The number of people for each compartment represents the states of a SIR epidemic model. The total number of individuals who are assumed to be mixed homogenously remains the same, which means the probability of each individual coming in contact with others is equal [3].

However, the generic SIR epidemic model must be expanded to include a fourth compartment in case of many infectious diseases, for instance, influenza-like illness, tuberculosis, and HIV/AIDS [3,9,10]. The state of the fourth compartment corresponds to the latency period of disease, i.e., someone who is infected but still unable to infect others. This modified model is called the SEIR epidemic model [11]. Several estimation techniques have been developed to track and estimate the states of these models [3,12,13]. To design these estimators to converge to actual states, one needs to know the exact values of the uncertain quantities. However, designing such estimators for SEIR models in a real scenario is challenging, especially when the uncertain parameters are not exactly known but are defined by an interval or polytope. Interval estimator techniques can solve such issues [14–22]. Based on the monotone system theory (MST), interval estimators are designed to estimate the real states at any time instant and generate a set of acceptable values known as the interval in [20,23–28]. The ability to deal with large and unknown uncertainties in the system is one of the key advantages of interval state estimator design [29–31]. However, getting cooperative/nonnegative systems are not always possible, and solving this issue for interval estimator design is still an open area of research.

This article proposes an interval estimation-based method to track and estimate the four states of the SEIR epidemic model subject to uncertain parameters. Diaby et al., 2015 [32] proposed the first interval estimator for the continuous-time epidemic model. The results obtained by Diaby et al. were adequate but not ideal because the observer gain was manually set. Instead, we consider the discrete-time SEIR model and use an efficient method based on the observability matrix to design the interval estimator without observer gain. Finite-time convergence for the interval vectors' width is derived to verify the boundedness of the estimation error that significantly improves the accuracy of the designed method.

It is worth mentioning that the observer gain used in the conventional interval observers' design determines the magnitude of the upper bound of the interval estimation errors (for instance, see [27,28]). As a result, interval observers that converge faster may result in a state enclosure that is too conservative at steady state. The noted issue is solved in this study since we do not require an observer gain to run the proposed state estimator. In contrast, set-membership state estimators address the optimization problem at each iteration, and the problem of finite convergence time is ignored. Therefore, the proposed result on finite time convergence is intriguing. However, it is a little more demanding in terms of computation time. Furthermore, compared with the Kalman filter-type estimators, the proposed interval state estimator requires less information on state disturbances and measurement noise to generate guaranteed enclosures of the real state vector. This knowledge is advantageous when dealing with real-world situations when state disturbances and measurement noise are poorly known. More specifically, compared with the existing results in the literature, the contributions are fourfold:

1. We solve the interval estimation problem for the fourth-order SEIR epidemic model subject to disturbances and uncertainties. The estimation procedure is designed based on the observability matrix to relax the strong cooperativity assumption for designing traditional interval observers. Finite-time convergence and tight initialization problems are analyzed separately to improve the performance of the developed method;

2. In contrast to the existing interval observer design methods [19,33], we considered a nonlinear model with unknown input affecting the output with a highly uncertain state matrix A. The bounds on the uncertain input are constructed before designing the interval estimator;
3. We introduce a novel interval state estimation method using an observability matrix and past input-output values without designing an observer gain that can alleviate some limitations of traditional interval observer design. For example, the system being cooperative/non-negative [20,34–39] and the probable inflation existence of the estimation error at the steady-state are avoided.
4. We consider the fourth compartment of the SEIR model by following the incubation stage compared with the interval estimator designed for the SIR model in [40]. Moreover, ref. [40] considered continuous-time dynamics, whereas we concentrate on the discrete time, which has grown in prominence through past years [41,42]. In addition, ref. [40] assumed that exact values of $\wp SI$ (new infectives per day) and the upper and lower bound of $\wp$ (transmission rate) are available. In our case, only noisy values of susceptible people S and probable bounds on uncertain $\wp SI$ are available, while the bounds on $\wp$ are not given by PHS. Hence, our method is more applicable in reality as $\wp$ is highly uncertain and cannot be obtained directly from biological consideration compared with [43,44]. Furthermore, its bounds are usually unavailable for such models [14].

The remainder of this work continues with notations and interval analysis in Section 2. The problem statement is described in Section 3, and the key findings are shown in Section 4. Two numerical examples are given in Section 5, where a comparison with previous results in [27,28] is demonstrated. Finally, concluding remarks are presented in Section 6.

2. Preliminaries Results

First, we reviewed some basic notations on interval estimation necessary to design the proposed state estimator.

2.1. Notations

A set of real numbers is symbolized by $\mathbb{R}$ with $\mathbb{R}_+ = \{\iota \in \mathbb{R} : \iota \geq 0\}$, whereas $\mathbb{Z}$ denotes a set of integers with $\mathbb{Z}_+ = \mathbb{Z} \cap \mathbb{R}_+$. The identity matrix of dimension n is denoted by $\mathbb{I}_n$. $\lambda_{\max}(\Delta)$ is the largest and $\lambda_{\min}(\Delta)$ is the smallest eigenvalue for a square matrix $\Delta \in \mathbb{R}^{n\times n}$. Let the L_2-induced matrix norm be $\|\Delta\|_2 = \sqrt{\lambda_{\max}(\Delta^T\Delta)}$, where the infinity norm is $\|\Delta\|_\infty = \max\limits_{1\leq i\leq n} \Sigma_{j=1}^{n} |a_{ij}|$. Δ is non-negative ($\Delta > 0$) if $a_{ij} \geq 0$, whereas it is Schur stable if $|\lambda_i| < 1$ for all $i, j = 1, \ldots, n$. The relations $\Delta_1 \leq \Delta_2$ and $\nabla_1 \leq \nabla_2$ are understood elementwise for two matrices $\Delta_1,\ \Delta_2 \in \mathbb{R}^{n\times n}$ or vectors $\nabla_1,\ \nabla_2 \in \mathbb{R}^n$. For known $A \in \mathbb{R}^{m\times n}$, we define $A^+ = \{0, A\}$ and $A^- = \{0, -A\}$ with $|A| = A^+ + A^-$.

2.2. Interval Analysis

Uncertain parameters are defined by intervals that contain real values of unknown variables in a guaranteed way.

Definition 1. *An interval vector $[x]$ is determined by [45]*

$$[x] = [\underline{x}, \overline{x}] = \{a | \underline{x} \leq a \leq \overline{x},\ \underline{x}, \overline{x} \in \mathbb{R}^n\}.$$

Lemma 1. *Let $x \in \mathbb{R}^n$ be an interval vector for some $\underline{x}, \overline{x} \in \mathbb{R}^n$ and $A \in \mathbb{R}^{m\times n}$. Then [29]*

$$A^+\underline{x} - A^-\overline{x} \leq Ax \leq A^+\overline{x} - A^-\underline{x}.$$

Definition 2. *The theory of monotone systems states that the solutions to the below system for given $x(0) \geq 0$ constructed by a matrix $A \in \mathbb{R}_+^n$ are non-negative,*

$$x(k+1) = Ax(k) + w(k),$$
$$x \in \mathbb{R}^n,\ w : \mathbb{Z}_+ \to \mathbb{R}_+^n,\ k \in \mathbb{Z}_+,\ k \geq 0$$

and the system is referred to as cooperative or non-negative [46].

3. Problem Statement

The SEIR discrete-time model demonstrated by Figure 1 and obtained using Euler discretization of the classical continuous-time model is given as follows [42,46]:

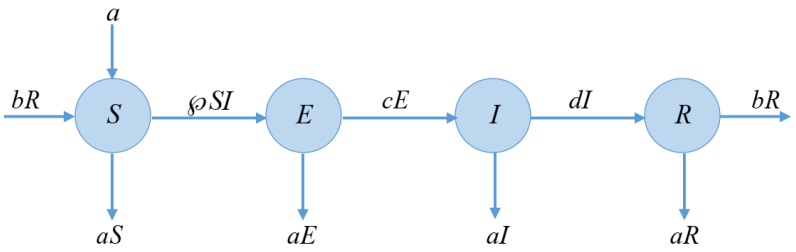

Figure 1. Block diagram for SEIR model.

$$\begin{aligned} S(k+1) &= (1-a(k))S(k) + b(k)R(k) - \wp(k)S(k)I(k) + a(k), \\ E(k+1) &= (1-a(k)-c(k))E(k) + \wp(k)S(k)I(k), \\ I(k+1) &= c(k)E(k) + (1-a(k)-d(k))I(k), \\ R(k+1) &= d(k)I(k) + (1-a(k)-b(k))R(k), \end{aligned} \tag{1}$$

where $S(k)$, $E(k), I(k), and R(k)$ represent state variables corresponding to the portion of population in each compartment of the model. The time-varying non-negative parameters a stands for the natural birth-death rate, whereas b, c, d denote the uncertain transition rates from one disease state to the other. The exact values of non-negative parameters a, b, c, d are unknown. We only know the lower bound and upper bound values, i.e., $a \in [\underline{a},\ \overline{a}]$, $b \in [\underline{b},\ \overline{b}]$, $c \in [\underline{c},\ \overline{c}]$ and $d \in [\underline{d},\ \overline{d}]$ with given $\underline{a}, \overline{a}, \underline{b}, \overline{b}, \underline{c}, \overline{c}, \underline{d}, \overline{d} \in \mathbb{R}_+$. The time-varying parameter $\wp(k)$ is extremely uncertain, and no bounds on $\wp(k)$ are available for measurements. The initial values for $x(k) \in \mathbb{R}^4$ are unknown but bounded with known bounds $\underline{x}(0), \overline{x}(0) \in \mathbb{R}^4$ such that $\underline{x}(0) \leq x(0) \leq \overline{x}(0)$. At at any given time instant k, the death rate is exactly equal to birth rate $a(k)$ in all the compartments. In fact, by summing up (1), one gets directly that the total population is constant, thus satisfying

$$N(k+1) = N(k) = N_0 \quad \forall k \in \mathbb{Z}_{0+},$$

for

$$N(k) = S(k) + E(k) + I(k) + R(k), \quad \forall k \in \mathbb{Z}_{0+}.$$

This results in

$$S(k+1) + E(k+1) + I(k+1) + R(k+1) = (1-a(k))N_0 + a(k), \quad \forall k \in \mathbb{Z}_{0+}.$$

Hence, if the total population is initially in unity, then (1) remains as a normalized model for all samples with the total population remaining in unity through time; therefore

$$S(k+1) + E(k+1) + I(k+1) + R(k+1) = 1 - a(k) + a(k) = 1, \quad \forall k \in \mathbb{Z}_{0+}. \tag{2}$$

The transmission of disease arises because of the interactions among susceptible and infectious individuals as described by (1). The disease is transferred to $\wp(k)$ individuals through infectious individuals at each time instant. However, a new case only arises with probability $S(k)$ when contact is directly made with the susceptible individual. Therefore,

in compartment S, a fraction $\wp(k)I(k)$ of people shift to exposed but non-infectious compartment E at time k. Similarly, a fraction c and d of individuals in compartments E and I migrate to the infectious I and recovered R compartments, respectively. It should be noted that the recovered compartment is composed of people not yet immune.

The output measured data consists of noisy counts of susceptible individuals obtained from different government sources such as census bureaus by PHS and are represented by the following output system model [3]:

$$y(k) = S(k) + v(k) \tag{3}$$

where $v(k) \in L_\infty$ stands for unknown measurement noise with known bounds $\underline{v}(k)$, $\overline{v}(k) \in L_\infty$ such that $\underline{v}(k) \leq v(k) \leq \overline{v}(k)$, $\forall k \geq 0$. The unknown measurement noise consists of the uncertain number of susceptible people who did not visit the health care unit for diagnosis. Therefore, Equations (1) and (3) are rewritten as follows:

$$\begin{aligned} x(k+1) &= A(k)x(k) + E\Im(k) + w(k), \\ y(k) &= Cx(k) + v(k), \end{aligned} \tag{4}$$

where $x(k) = [S(k)\ E(k)\ I(k)\ R(k)]^T$ and $\Im(k) = \wp(k)S(k)I(k)$ represent the unknown state vector to be determined and uncertain input, i.e., the newly confirmed infected people from the susceptible individuals at each time instant in the known population, respectively. The time-varying unknown matrix $A(k)$ and constant matrices E and C in (4) are given by

$$A(k) = \begin{bmatrix} 1-a & 0 & 0 & b \\ 0 & 1-a-c & 0 & 0 \\ 0 & c & 1-a-d & 0 \\ 0 & 0 & d & 1-a-b \end{bmatrix},$$

$$E = \begin{bmatrix} -1 \\ 1 \\ 0 \\ 0 \end{bmatrix},\ w(k) = \begin{bmatrix} a(k) \\ 0 \\ 0 \\ 0 \end{bmatrix},\ C = \begin{bmatrix} 1 \\ 0 \\ 0 \\ 0 \end{bmatrix}^T.$$

The uncertain unknown bounded matrix $w(k)$ for $\underline{w}, \overline{w} \in L_\infty$ is defined as

$$\underline{w} = \begin{bmatrix} \underline{a}(k) \\ 0 \\ 0 \\ 0 \end{bmatrix},\ \overline{w} = \begin{bmatrix} \overline{a}(k) \\ 0 \\ 0 \\ 0 \end{bmatrix},$$

such that $\underline{w} \leq w \leq \overline{w}$.

4. Interval Estimator Design for SEIR Model

We will design the interval state estimator in this section for the SEIR model (4). In the presence of uncertain parameters, the primary goal of this research is to construct an interval estimator for the SEIR model such that the unknown state signals always satisfy the following inequality:

$$\underline{x}(k) \leq x(k) \leq \overline{x}(k),\ \forall k \geq 0, \tag{5}$$

where $\underline{x}(k), \overline{x}(k)$ represent the highest and lowest values for the interval state bounds provided that $x(0) \in [\underline{x}(0), \overline{x}(0)]$. The proposed interval estimator can help to make a deciding rule for pandemic detection. The following definition and assumption are required to design the proposed interval state estimator for the given SEIR model.

Proposition 1. *As the state $x(k_0) = x(0)$ is determined uniquely for all $u(\tau)$ and $y(\tau)$, $\tau \in [k_0, k_1]$, the SEIR epidemic model described by (4) is observable over $[k_0, k_1]$.*

Assumption 1. *There are known bounds* $\underline{w}, \overline{w} \in \mathbb{R}^4$, $\underline{v}, \overline{v} \in \mathbb{R}$ *such that* $w(k) \in [\underline{w}, \overline{w}]$, $v(k) \in [\underline{v}, \overline{v}]$.

The given proposition and assumption are necessary for designing the proposed interval estimator. The bounds given by Assumption 1 determine the uncertainty of initial values, input disturbance and noise.

4.1. Interval State Estimator Design

The observability matrix $\bigcirc \in \mathbb{R}^{4\times4}$ for (4) is given by

$$\bigcirc = \begin{bmatrix} C \\ CA(k) \\ CA(k+1)A(k) \\ CA(k+2)A(k+1)A(k) \end{bmatrix}$$

Then, the SEIR model (4) can be written in the input/output form in the absence of uncertain quantities and exogenous signals as follows:

$$\begin{aligned} x(k+4) &= A(k+3)A(k+2)A(k+1)A(k)x(k), \\ \begin{bmatrix} y(k) \\ y(k+1) \\ y(k+2) \\ y(k+3) \end{bmatrix} &= \Psi(k:k+3) = \bigcirc x(k). \end{aligned} \tag{6}$$

As a result, using available input-output values, (6) can be written as follows:

$$x(k) = \bigcirc^{-1}\Psi(k:k+3) \tag{7}$$

Hence, the states of the SEIR model (4) can be obtained using the available input/output values for $k-3 \geq 0$ by

$$\hat{x}(k) = \Delta_y(k)\Psi(k-3:k), \tag{8}$$

with

$$\Delta_y(k) = A(k-1)A(k-2)A(k-3)\bigcirc^{-1}.$$

Then, the equation of our interval state estimator for the SEIR model (4) that generates certain bounds on the real states for $k-3 \geq 0$ subject to exogenous signals takes the following form:

$$\begin{aligned} \overline{x}(k) &= \hat{x}(k) + \overline{D} + \overline{\Lambda}(k) + \overline{V}, \\ \underline{x}(k) &= \hat{x}(k) + \underline{D} + \underline{\Lambda}(k) + \underline{V}, \end{aligned} \tag{9}$$

where $\overline{D}, \underline{D} \in \mathbb{R}^{4\times1}$, $\overline{\Lambda}(k), \underline{\Lambda}(k) \in \mathbb{R}^{4\times1}$ and $\overline{V}, \underline{V} \in \mathbb{R}^{4\times1}$ denote the upper and lower limits on uncertain birth and death rate, uncertain input, and measurement noise, respectively. We will define these terms one by one using Lemma 1 as follows.

4.1.1. Bounds on the Uncertain Birth and Death Rate

The bounds of the unknown birth and death rate are given by

$$\begin{aligned} \overline{D} &= \phi^+(k)\overline{w}_{n-1} + \phi^-(k)\underline{w}_{n-1} \\ \underline{D} &= \phi^+(k)\underline{w}_{n-1} + \phi^-(k)\overline{w}_{n-1} \end{aligned}, \tag{10}$$

where $\overline{w}_{n-1} \in \mathbb{R}^{12\times1}$ and $\underline{w}_{n-1} \in \mathbb{R}^{12\times1}$ denote $n-1$ bound concatenation on the uncertain birth and death rate defined by

$$\overline{w}_{n-1} = \begin{bmatrix} \overline{w} & \overline{w} & \overline{w} \end{bmatrix}^T, \quad \underline{w}_{n-1} = \begin{bmatrix} \underline{w} & \underline{w} & \underline{w} \end{bmatrix}^T,$$

with

$$\overline{w} = \begin{bmatrix} \overline{a}(k) & 0 & 0 & 0 \end{bmatrix}^T, \quad \underline{w} = \begin{bmatrix} \underline{a}(k) & 0 & 0 & 0 \end{bmatrix}^T.$$

Furthermore,

$$\phi^+(k) = \max\{0,\ \phi(k)\},\ \phi^+(k) = \max\{0,\ -\phi(k)\},\ \phi(k) = \Sigma_A - \Delta_y(k)\Sigma_{CA},$$

where

$$\Sigma_A = \begin{bmatrix} \xi_{11} & 0 & \xi_{13} & \xi_{14} & \xi_{15} & 0 & 0 & \xi_{18} \\ 0 & \xi_{22} & 0 & 0 & 0 & \xi_{26} & 0 & 0 \\ 0 & \xi_{32} & \xi_{33} & 0 & 0 & \xi_{36} & \xi_{37} & 0 \\ 0 & \xi_{42} & \xi_{43} & \xi_{44} & 0 & 0 & \xi_{47} & \xi_{48} \end{bmatrix} \mathbb{I}_4, \tag{11a}$$

and

$$\begin{aligned}
&\xi_{11} = (1 - a(k_1))(1 - a(k_2)),\\
&\xi_{13} = b(k_1)d(k_2),\\
&\xi_{14} = b(k_2)(1 - a(k_1)) + b(k_1)(1 - a(k_2) - b(k_2)),\\
&\xi_{15} = (1 - a(k_2)),\\
&\xi_{18} = b(k_2),\\
&\xi_{22} = (1 - a(k_1) - c(k_1))(1 - a(k_2) - c(k_2)),\\
&\xi_{26} = (1 - a(k_2) - c(k_2)),\\
&\xi_{32} = c(k_2)(1 - a(k_1) - c(k_1)) + c(k_1)(1 - a(k_2) - c(k_2)),\\
&\xi_{33} = (1 - a(k_1) - d(k_1))(1 - a(k_2) - d(k_2)),\\
&\xi_{36} = c(k_2),\\
&\xi_{37} = (1 - a(k_2) - d(k_2)),\\
&\xi_{42} = d(k_1)c(k_2),\\
&\xi_{43} = d(k_2)(1 - a(k_1) - d(k_1)) + d(k_1)(1 - a(k_2) - d(k_2)),\\
&\xi_{44} = ((1 - a(k_1) - b(k_1))((1 - a(k_2) - b(k_2)),\\
&\xi_{47} = d(k_2),\\
&\xi_{48} = (1 - a(k_2) - b(k_2)),
\end{aligned}$$

$$\Sigma_{CA} = \begin{bmatrix} 0_{4\times1} & 0_{4\times1} & 0_{4\times1} \\ C & 0_{4\times1} & 0_{4\times1} \\ CA(k_1) & C & 0_{4\times1} \\ CA(k_1)A(k_2) & CA(k_1) & C \end{bmatrix},$$

$$= \begin{bmatrix} 0 & 0 & 0 & 0 \\ 1 & 0 & 0 & 0 \\ 1 - a(k_1) & 0 & 0 & b(k_1) \\ \{1 - a(k_1)\} & 0 & b(k_1) & -b(k_1)b(k_2) + \\ \{1 - a(k_2)\} & & d(k_1) & b(k_1)\{1 - a(k_1)\} + \\ & & & b(k_2)\{1 - a(k_1)\} \end{bmatrix}$$

$$\begin{bmatrix} 0 & 0 & 0 & 0 & 0 & 0 & 0 & 0 \\ 0 & 0 & 0 & 0 & 0 & 0 & 0 & 0 \\ 1 & 0 & 0 & 0 & 0 & 0 & 0 & 0 \\ 1 - a(k_1) & 0 & 0 & b(k_1) & 1 & 0 & 0 & 0 \end{bmatrix}, \tag{11b}$$

with $k_1 = k - 1,\ k_2 = k - 2$.

4.1.2. Bounds on Uncertain Input

The bounds on the uncertain input are represented as

$$\begin{array}{l} \overline{\Lambda}(k) = (\phi E_{n-1})^{+}\overline{\Im}(k) - (\phi E_{n-1})^{-}\underline{\Im}(k), \\ \underline{\Lambda}(k) = (\phi E_{n-1})^{+}\underline{\Im}(k) - (\phi E_{n-1})^{-}\overline{\Im}(k). \end{array} \tag{12}$$

Using (3) and (4), one can write

$$\begin{aligned} y(k+1) &= Cx(k+1) + v(k+1), \\ &= CA(k)x(k) + CE\Im(k) + Cw(k) + v(k+1), \end{aligned}$$

$$-CE\Im(k) = CA(k)x(k) + Cw(k) - y(k+1) + v(k+1).$$

Moreover, from (1), (3) and (4), we derive that

$$CE = -1,\ Cw(k) = a(k).$$

This results in

$$\Im(k) = CA(k)x(k) + a(k) - y(k+1) + v(k+1),$$

with

$$\begin{array}{l} \overline{\Im}(k) = (CA)^{+}\overline{x}(k) - (CA)^{-}\underline{x}(k) + |-y(k+1)| + \overline{v} + \overline{a} \\ \underline{\Im}(k) = (CA)^{+}\underline{x}(k) - (CA)^{-}\overline{x}(k) + |-y(k+1)| - \overline{v} + \underline{a} \end{array},$$

such that $[\Im(k)] = [\underline{\Im}(k),\ \overline{\Im}(k)]$ and $E_{n-1} = [E \quad E \quad E]^T$.

4.1.3. Bounds on Measurement Noise Vector

The bounds for the measurement noise vector are described by

$$\begin{array}{l} \overline{V} = \varphi_v^{+}(k)\overline{v}_n + \varphi_v^{-}(k)\underline{v}_n, \\ \underline{V} = \varphi_v^{+}(k)\underline{v}_n + \varphi_v^{-}(k)\overline{v}_n, \end{array} \tag{13}$$

where $\overline{v}_n,\ \underline{v}_n \in \mathbb{R}^{4\times 1}$, respectively, denote the n concatenation of $\overline{v} \in \mathbb{R}$ and $\underline{v} \in \mathbb{R}$, given by

$$\overline{v}_n = \begin{bmatrix} \overline{v} \\ \overline{v} \\ \overline{v} \\ \overline{v} \end{bmatrix}, \quad \underline{v}_n = \begin{bmatrix} \underline{v} \\ \underline{v} \\ \underline{v} \\ \underline{v} \end{bmatrix},$$

and

$$\varphi_v^{+}(k) = \max\{0,\ \varphi_v(k)\},\ \phi_v^{-}(k) = \max\{0,\ -\varphi_v(k)\}$$

with

$$\varphi_v(k) = -\Delta_y(k).$$

Theorem 1. *When Assumption 1 is satisfied for the given SEIR model (4), the interval state estimator given by (9) yields the following relations:*

$$\underline{x}(k) \le x(k) \le \overline{x}(k), \quad \forall k \ge 3, \tag{14}$$

provided that $\underline{x}(0) \le x(0) \le \overline{x}(0)$.

Proof of Theorem 1. The solution to the SEIR model (4) at any time instant k for $x(0) \in [\underline{x}(0), \overline{x}(0)]$ and $w(k) \in [\underline{w}, \overline{w}]$ can be obtained as

$$x(k) = \prod_{\ell=1}^{k} A(k-\ell)x(0) + E\Im(k-1) + w(k-1) + \sum_{m=0}^{k-2}\left\{\prod_{\ell=1}^{k-m-1} A(k-\ell)\right\}\{E\Im(m) + w(m)\}. \tag{15}$$

The given SEIR model is a 4th order system i.e., $n = 4$. Therefore, the states $x(k)$ can be determined at any time k using previous state values at $k-3$ as follows:

$$\begin{aligned} x(k) = {} & A(k-1)A(k-2)A(k-3)x(k-3) + A(k-1)A(k-2)\{E\Im(k-3) + w(k-3)\} \\ & + A(k-1)\{E\Im(k-2) + w(k-2)\} + E\Im(k-1) + w(k-1). \end{aligned} \tag{16}$$

Now using theory of interval analysis [39] for all $x(k-3) \in [x(k-3)]$, $\Im(\vartheta) \in [\Im(\vartheta)]$ and $w(\vartheta) \in [w(\vartheta)]$ with $\vartheta \in \{k-3,\ k-2,\ k-1\}$, the state vector $x(k) \in [x(k)]$ is given by

$$[x(k)] = A(k-1)A(k-2)A(k-3)[x(k-3)] + \Sigma_A\{E_{n-1}[\Im(k)] + [w_{n-1}]\}, \tag{17}$$

As a result, utilizing the past input/output values and the observability matrix, the following set inversion formula is obtained to get the state enclosure $[x(k-3)]$:

$$[x(k-3)] = \bigcirc^{-1}\{[\Psi(k-3:k)] - \Sigma_{CA}E_{n-1}[\Im(k)]\} + \bigcirc^{-1}\Sigma_{CA}[w_{n-1}], \tag{18}$$

where

$$[\Psi(k-3:k)] = \begin{bmatrix} y(k-3) \\ y(k-2) \\ y(k-1) \\ y(k) \end{bmatrix} - [v_n].$$

Consequently, by combing (17) and (18), one gets

$$\begin{aligned} [x(k)] = {} & A(k-1)A(k-2)A(k-3)\bigcirc^{-1}([\Psi(k-3:k)] - \Sigma_{CA}\{E_{n-1}[\Im(k)] + [w_{n-1}]\}) \\ & + \Sigma_A\{E_{n-1}[\Im(k)] + [w_{n-1}]\}, \end{aligned} \tag{19}$$

$$\begin{aligned} [x(k)] = {} & \Delta_y(k)\{[\Psi(k-3:k)] - [v_n]\} - \Delta_y(k)\Sigma_{CA}\{E_{n-1}[\Im(k)] + [w_{n-1}]\} \\ & + \Sigma_A\{E_{n-1}[\Im(k)] + [w_{n-1}]\}, \end{aligned} \tag{20}$$

$$[x(k)] = \Delta_y(k)[\Psi(k-3:k)] - \Delta_y(k)[v_n] + (\Sigma_A - \Delta_y(k)\Sigma_{CA})\{E_{n-1}[\Im(k)] + [w_{n-1}]\}, \tag{21}$$

$$[x(k)] = \Delta_y(k)[\Psi(k-3:k)] + \phi(k)E_{n-1}[\Im(k)] + \phi(k)[w_{n-1}] + \varphi_v(k)[v_n], \tag{22}$$

$$[x(k)] = \hat{x}(k) + [\Lambda] + [D] + [V], \tag{23}$$

where $[x(k)] = [\underline{x}, \overline{x}]$, $[\Lambda] = [\underline{\Lambda}, \overline{\Lambda}]$, $[D] = [\underline{D}, \overline{D}]$ and $[V] = [\underline{V}, \overline{V}]$. This completes the proof of Theorem 1. □

4.2. Interval Prediction for $k < 3$

It is worth mentioning that to use the developed interval state estimator (9) for the given SEIR model (4), the initial $n-1 = 3$ values of input-output should be accessible. However, in many real life scenarios, these values are not always available for measurements, such as in the given case, where only the initial values are given with some known bounds. Therefore, we proposed the following recursive system as an interval predictor that provides a bound on the system's states for $k = 0, 1, 2$.

Proposition 2. *The following interval predictor generates $[x(k)]$ such that for $k = 0, 1, 2$, we have $x(k) \in [x(k)]$ as*

$$\begin{aligned} [x(k)] &= \textstyle\prod_{\ell=1}^{k} A(k-\ell)[x(0)] + [\partial(k-1)], \\ [\partial(k)] &= A(k)[\partial(k-1)] + E[\Im] + [w], \\ [\partial(0)] &= E[\Im] + [w]. \end{aligned} \tag{24}$$

Proof. To prove Proposition 2, we use mathematical induction. As for the initial case $k = 0$, the input and output are available. Therefore, we consider the case $k = 1$. Hence, the first cycle of the SEIR model produces the following equations:

$$\begin{array}{l} x(1) = A(0)x(0) + E\Im(0) + w(0), \\ [x(1)] \in A(0)[x(0)] + E[\Im] + [w], \\ [x(1)] \in A(0)[x(0)] + [\partial(0)], \end{array} \tag{25}$$

which implies the correctness of (24) for $k = 1$. Next, we demonstrate that (24) is true for $k = 2$. Once again, considering (4) for $k = 2$, we get

$$\begin{array}{l} x(2) = \prod_{\ell=1}^{2} A(2-\ell)x(0) + E\Im(1) + w(1) + \sum_{m=0}^{1}\left\{\prod_{\ell=1}^{2} A(2-\ell)\right\}\{E\Im(m) + w(m)\}, \\ [x(2)] \in \prod_{\ell=1}^{2} A(2-\ell)[x(0)] + A(1)[\partial(0)] + E[\Im] + [w], \end{array} \tag{26}$$

$$[x(2)] \in \prod_{\ell=1}^{2} A(2-\ell)[x(0)] + [\partial(1)]. \tag{27}$$

Thus, by simple mathematical induction, one can easily show that (27) is true for $k = 2$ as well. This completes the proof of Proposition 2. □

4.3. Finite-Time Convergence

The finite-time convergence of the interval width $\mho[x(k)]$ is one of the primary issues concerning the tight initialization and stability of the interval estimator. Therefore, this section proves that $\mho[x(k)]$ converges to a known upper-bounded value in finite time provided by the uncertain quantities. Hence, we introduce the following Lemma to compute the upper bound on $\mho[x(k)]$.

Lemma 2. *The following inequality determines the upper bound on the width of the interval vector provided by (9) and (24):*

$$\mho[x(k)] \leq \|\phi(k)E_{n-1}\|_\infty \mho[\Im] + \|\phi(k)\|_\infty \mho[w] + \|\varphi_v(k)\|_\infty \mho[v_n], \quad \forall k \geq 3. \tag{28}$$

Proof. Firstly, the recursive system (24) is employed as an interval predictor during the initialization phase for $k = 0, 1, 2$ to provide tight bounds on the interval vector of the SEIR model (4). As a result, the upper limit on the width of interval vector provided by (24) is given by

$$\mho[x(k)] \leq \left\| \prod_{\ell=1}^{k} A(k-\ell) \right\|_\infty \mho[x(0)] + \mho[\partial(k-1)]. \tag{29}$$

Secondly, the proposed interval state estimator (9) is used for $k \geq 3$. Then, Equation (23) implies

$$\mho[x(k)] \leq \|\phi(k)E_{n-1}\|_\infty \mho[\Im] + \|\phi(k)\|_\infty \mho[w_{n-1}] + \|\varphi_v(k)\|_\infty \mho[v_n], \tag{30}$$

whereas

$$\begin{array}{l} \|\phi(k)E_{n-1}\|_\infty \mho[\Im] + \|\phi(k)\|_\infty \mho[w_{n-1}] + \|\varphi_v(k)\|_\infty \mho[v_n] \\ \leq \|\phi(k)E_{n-1}\|_\infty \mho[\Im] + \|\phi(k)\|_\infty \mho[w] + \|\varphi_v(k)\|_\infty \mho[v_n]. \end{array} \tag{31}$$

Based on (30) and (31), one can easily determine that

$$\mho[x(k)] \leq \|\phi(k)E_{n-1}\|_\infty \mho[\Im] + \|\phi(k)\|_\infty \mho[w] + \|\varphi_v(k)\|_\infty \mho[v_n]. \tag{32}$$

This completes the proof of Lemma 2. □

Remark 1. *It is worth noting that we do not need observer gain to design the interval estimator. Therefore, the impact of gain that leads to pessimistic state enclosures for the traditional-type interval observer design method [27,28] is avoided. However, it is more demanding in term of computation*

time. In addition, unlike Kalman filter-type state estimators, the exact values of exogenous signals are not necessarily known and hence represent an advantage while dealing with practical applications.

5. Simulation Results

In this section, two simulated examples are used to demonstrate the efficiency of the designed interval state estimator compared with the traditional interval observer design methods [27,28]. Example 1 is a general numerical type, whereas Example 2 is based on the 2014 West African Ebola virus outbreak [47].

5.1. Example 1

Consider the SEIR epidemic model (4) with the following parameters defining the time-varying matrix $A(k)$ as

$$\begin{aligned} a(k) &= a(0) + 0.05\sin(0.5\pi k) \\ b(k) &= b(0) + 0.02\sin(0.5\pi k) \\ c(k) &= c(0) + 0.1\sin^2(0.25\pi k) \\ d(k) &= d(0) + 0.1\sin(0.25\pi k) \end{aligned}$$

with $a(0) = 0.4/\text{month}$, $b(0) = 0.124/\text{month}$, $c(0) = 0.2/\text{month}$, $d(0) = 0.45/\text{month}$ and degree of seasonality $\eta = 0.4$.

The uncertain input parameter is $\wp(k) = 0.5(1 + \eta\cos(0.25k))$, while the bounded disturbance and output measurement noise are: $w(k) \in [\underline{w}(k)\ \overline{w}(k)]$ for $\underline{w}(k) = [0.35\ 0\ 0\ 0]^T$, $\overline{w}(k) = [0.45\ 0\ 0\ 0]^T$ and $v(k) = V\cos(0.25\pi k)$ with $V = -0.00001$.

The two matrices Σ_A and Σ_{CA} are, respectively, obtained using (12a) and (12b), and bounds on the uncertain quantities are calculated by (10), (11) and (13). The observability matrix for $\kappa_j = (k + j);\ j = 0, 1, 2$ is computed as follows:

$$\bigcirc^{-1} = \begin{bmatrix} 1 & 0 & 0 \\ 1 - a_{\kappa_0} & 0 & 0 \\ (1 - a_{\kappa_1})(1 - a_{\kappa_0}) & 0 & b_{\kappa_1} d_{\kappa_0} \\ (1 - a_{\kappa_2})(1 - a_{\kappa_1})(1 - a_{\kappa_0}) & b_{\kappa_1} c_{\kappa_0} d_{\kappa_2} & \begin{array}{l} b_{\kappa_1} d_{\kappa_2}(1 - a_{\kappa_0} - d_{\kappa_0}) \\ +d_{\kappa_0}\{b_{\kappa_1}(1 - a_{\kappa_2}) \\ +b_{\kappa_2}(1 - a_{\kappa_1} - b_{\kappa_1}) \end{array} \end{bmatrix}$$

$$\begin{bmatrix} 0 \\ b_{(\kappa_0)} \\ (1 - a_{(\kappa_1)})b_{(\kappa_0)} + b_{(\kappa_1)}(1 - a_{(\kappa_0)} - b_{(\kappa_0)}) \\ b_{\kappa_0}(1 - a_{\kappa_2})(1 - a_{\kappa_1}) + (1 - a_{\kappa_0} - b_{\kappa_0}) \{b_{\kappa_1}(1 - a_{\kappa_2}) + b_{\kappa_2}(1 - a_{\kappa_1} - b_{\kappa_1})\} \end{bmatrix}$$

It should be noted that our model is of order four, i.e., $n = 4$. Therefore, we need to know the first two state intervals to implement the given interval estimator (9) for $k \geq 3$. Hence, the interval predictor (24) is used for $k = 1, 2$ provided that the initial values $\underline{x}(0) \leq x(0) \leq \overline{x}(0)$ are satisfied. It is worth mentioning that the given model does not have to be non-negative for the proposed interval estimator to operate.

Simulation experiments of the proposed method and the one in [28] are conducted to show the efficiency of the given approach. As perceived, the actual states are confined inside the two boundaries generated by (24) and (9). Figure 2 depicts the evolution of the actual states $x_s,\ s = 1, 2, 3, 4$, the estimated bounds by the proposed method (solid pink

lines), and the estimated bounds by MST (blue dashed line) [28]. The figure shows that the developed approach estimates tighter bounds than those calculated using the method described in [28]. Furthermore, in regards to the design perspective, the observer gain matrix in [28] needs to be Schur and non-negative, while we do not need an observer gain to design the interval estimator.

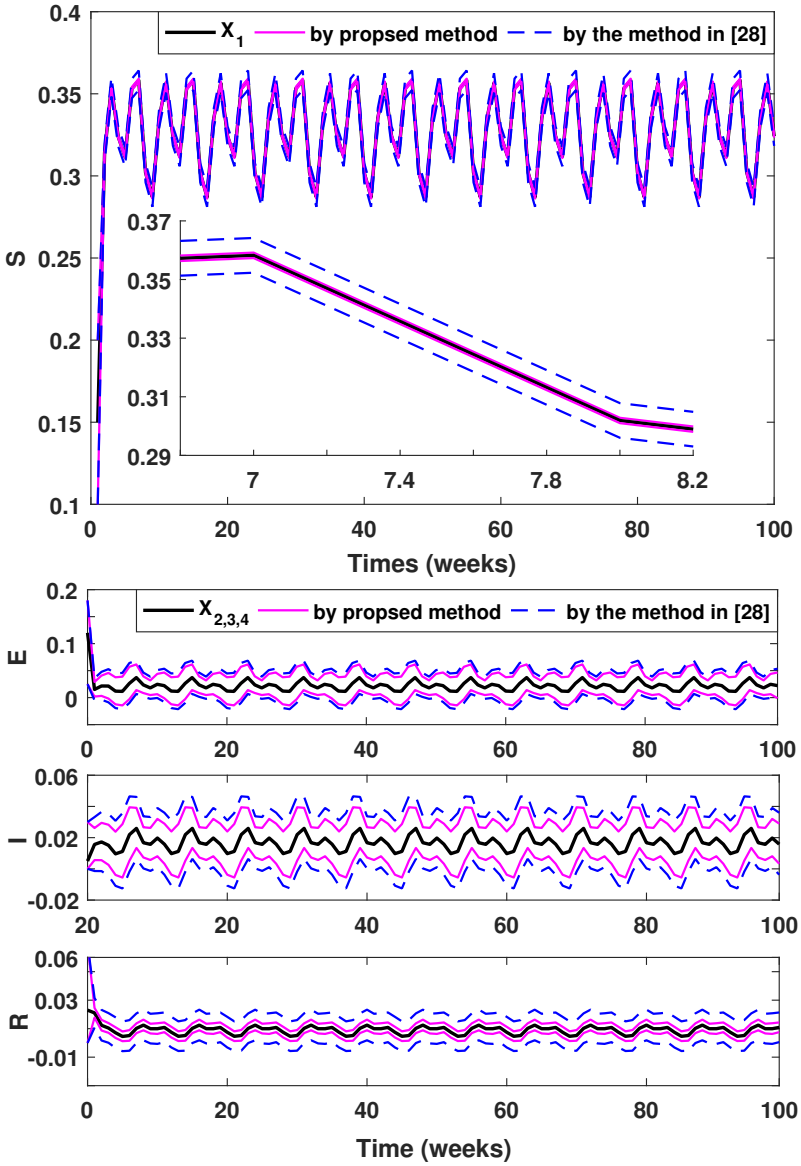

Figure 2. Interval estimations by proposed method vs. given in [28] for each state variable x_1, x_2, x_3, x_4 corresponding to S, E, I, R.

Secondly, the comparison of the interval state estimation errors e_S, e_E, e_I and e_R reflected in Figures 3 and 4 further clarify that the estimated bounds generated by the proposed method are more accurate and precise compared with [28]. Finally, Figure 5 shows the convergence of the interval widths given by (28). After three steps, the interval widths converge to their final values, proving the finite-time convergence performance of the proposed technique. Thus, it is concluded that the proposed method has a better performance.

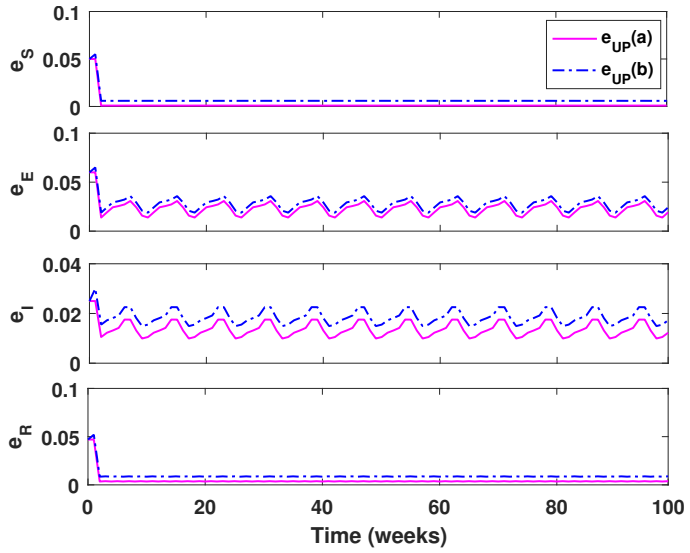

Figure 3. Upper-bound error: (a) proposed method; (b) method given in [28].

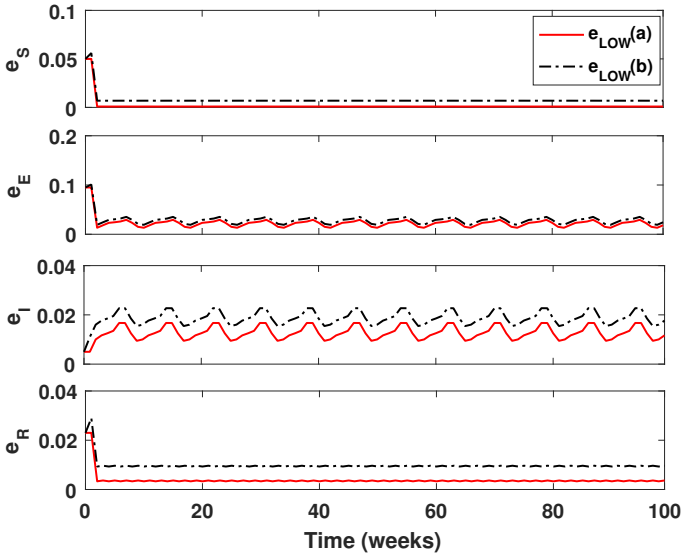

Figure 4. Lower-bound error: (a) proposed method; (b) method given in [28].

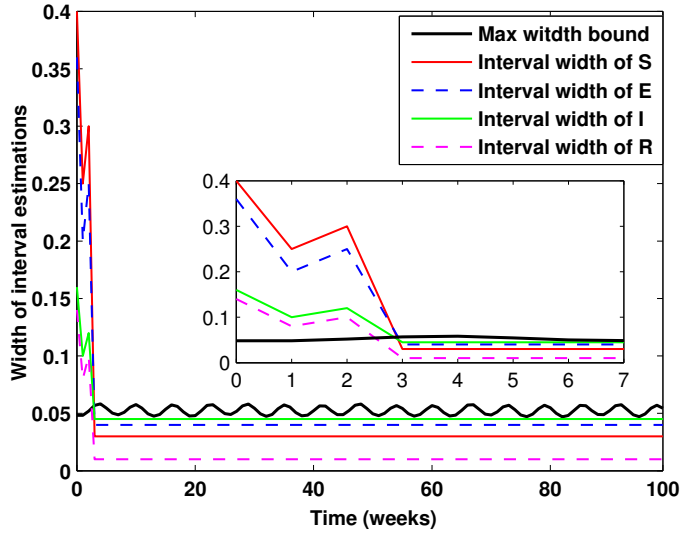

Figure 5. Finite-time convergence of S, E, I and R after 3rd iteration.

5.2. Example 2: Ebola Outbreak in West Africa

The 2014 West Africa Ebola outbreak [47] is considered using the following parameters to demonstrate the efficiency of the suggested technique having a period of one day as

$$a = 0.0099/day,\ b = 0.00128/day,\ c = 0.1887/day,$$
$$d = 0.1/day,\ \wp = 0.4/day.$$

Using these parameters, we get matrix A, as follows:

$$A = \begin{bmatrix} 0.9901 & 0 & 0 & 0.00128 \\ 0 & 0.8014 & 0 & 0 \\ 0 & 0.1887 & 0.8901 & 0 \\ 0 & 0 & 0.1 & 0.9888 \end{bmatrix}.$$

The output measurement noise $v(k)$ is uniformly distributed with given bounds

$$-V \leq v(k) \leq V; \quad V = 0.001.$$

We assumed that $\Im(k) = \wp S(y - v)$ is unknown but bounded with the following constraints:

$$\Im(k) - \tau = \underline{\Im}(k) \leq \Im(k) \leq \overline{\Im}(k) = \Im(k) + \tau; \quad \tau = 0.0001.$$

The observability matrix is obtained using A and C as

$$\bigcirc = \begin{bmatrix} 1 & 0 & 1 & 0 \\ 0.9991 & 0.1887 & 0.8991 & 0.0013 \\ 0.9982 & 0.3226 & 0.8085 & 0.0026 \\ 0.9973 & 0.4140 & 0.7272 & 0.0038 \end{bmatrix}.$$

The disturbance matrix to obtain bounds on the uncertain input, and uncertain birth and death rate is computed as
$\phi(k) = \Sigma_A - \Delta_y(k)\Sigma_{CA}$ with $\Delta_y(k) = A^3 \bigcirc^{-1}$ and

$$\Sigma_A = \begin{bmatrix} 0.9696 & 0 & 0.0001 & 0.0024 & 0.96 & 0 & 0 & 0 & 1 & 0 & 0 & 0 \\ 0 & 0.5016 & 0 & 0 & 0 & 0.66 & 0.66 & 0 & 0 & 1 & 0 & 0 \\ 0 & 0.4348 & 0.7638 & 0 & 0 & 0.3 & 0.8493 & 0 & 0 & 0 & 1 & 0 \\ 0 & 0.0332 & 0.2057 & 0.9672 & 0 & 0 & 0.1107 & 0.9588 & 0 & 0 & 0 & 1 \end{bmatrix},$$

$$\Sigma_{CA} = \begin{bmatrix} 0 & 0 & 0 & 0 & 0 & 0 & 0 & 0 & 0 & 0 & 0 & 0 \\ 1 & 0 & 0 & 0 & 0 & 0 & 0 & 0 & 0 & 0 & 0 & 0 \\ 1.01 & 0 & 0 & 0.0012 & 1 & 0 & 0 & 0 & 0 & 0 & 0 & 0 \\ 0.9696 & 0 & 0.0001 & 0.0024 & 1.01 & 0 & 0 & 0.0012 & 1 & 0 & 1 & 0 \end{bmatrix}.$$

Similarly, the measurement noise matrix is calculated as $\varphi_v(k) = -\Delta_y(k)$. The initial unknown bounded states are part of the interval $\underline{x}(0) \leq x(0) \leq \overline{x}(0)$ with $\underline{x}(0) = [0.88\ 0.06\ 0.049\ 0]$ and $\overline{x}(0) = [0.93\ 0.08\ 0.052\ 0.05]$.

The bounds on the uncertain input, uncertain birth-death rate and measurement noise are obtained using (10), (11) and (13), respectively. For the proposed SEIR model (4), we have $n = 4$; therefore, interval predictor (24) is used for $k = 1, 2$ whereas (9) is used for $k > 2$ to obtain guaranteed bounds on $x(k)$ provided that $\underline{x}(0) \leq x(0) \leq \overline{x}(0)$.

The simulation results of the proposed method and the one in [27] are depicted in Figure 6 to compare the observers' dynamics. As shown in Figure 6, the bounds generated by the developed method are tighter than those resulting from the work of Degue et al. [27]. In addition, the proposed method is easy to implement compared with [27] as it does not need observer gain and nonnegativity of the system dynamics to design the interval estimator. Moreover, Figures 7 and 8 show that the interval estimation errors $e_i^- = \underline{x}_r - x_r$,

$e_i^+ = \overline{x}_r - x_r$ for $r = 1, 2, 3, 4$; $i = S, E, I, R$, respectively, provided by our work are much smaller compared with [27].

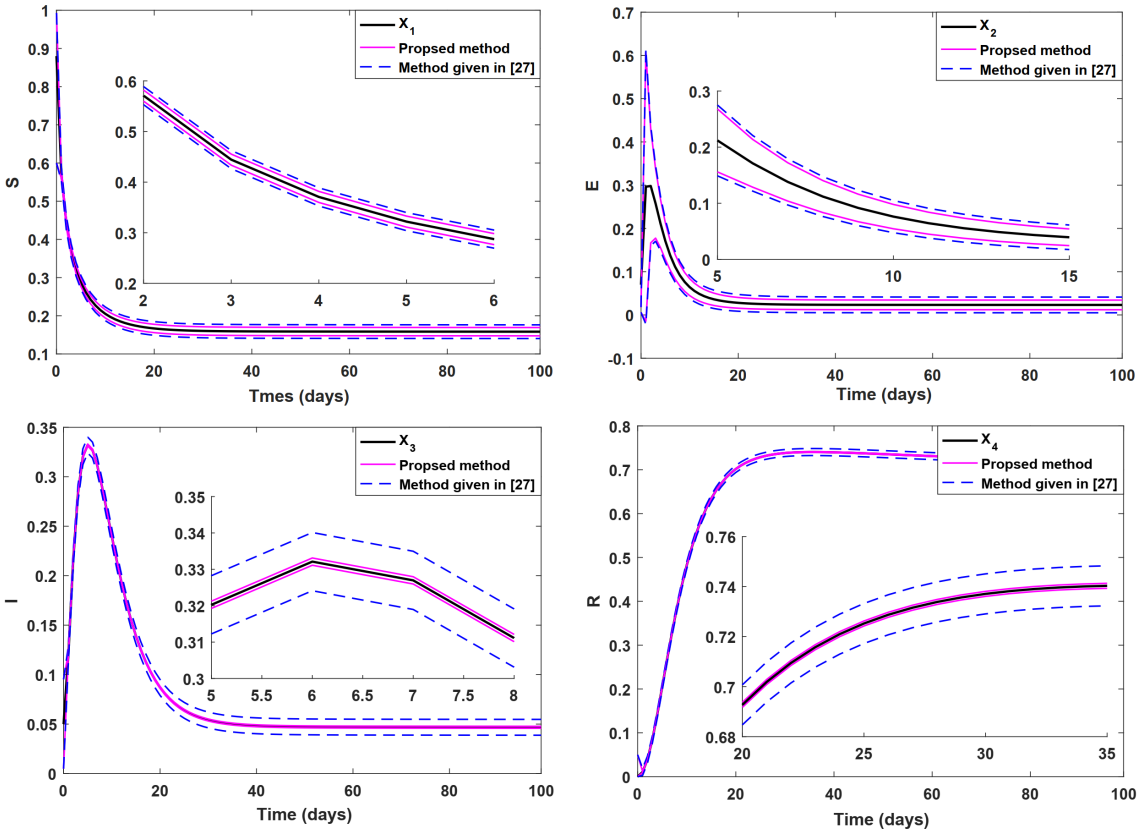

Figure 6. Interval estimations by proposed method vs. the method given in [27] for each state variable x_1, x_2, x_3, x_4 corresponding to S, E, I, R.

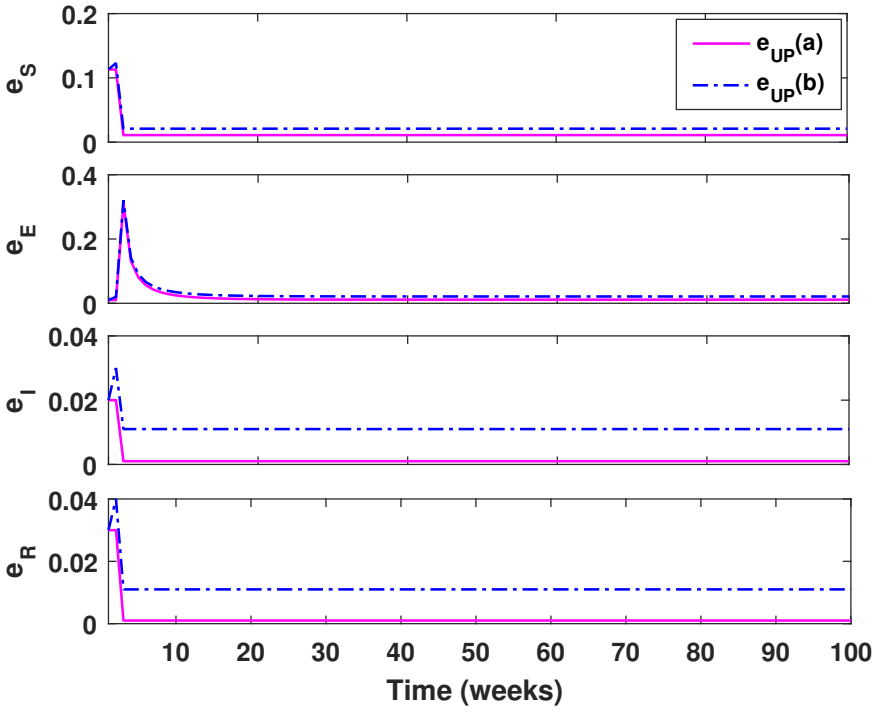

Figure 7. Upper-bound error: (a) proposed method; (b) method given in [27].

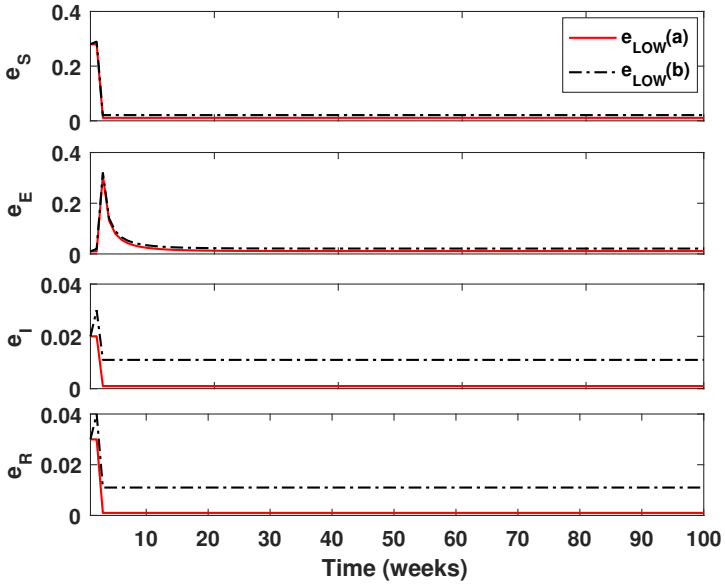

Figure 8. Lower-bound error: (a) proposed method; (b) method given in [27].

6. Conclusions

We developed a new strategy to design an interval state estimator for a fourth-order nonlinear discrete-time SEIR epidemic model subject to uncertain input, disturbances and measurement noise. The proposed method only requires the bounded values instead of exact values for state disturbance, unknown input, and parameters. In addition, no bounds on the time-varying transmission rate (susceptible to the infected stage) are required. The MST is widely used to design such an observer, but obtaining a non-negative model is not always feasible. Therefore, the proposed interval state estimator relaxes such restrictions by estimating the four compartment states using the observability matrix instead of point-wise estimation. The finite-time convergence of the interval width for the proposed approach is investigated to demonstrate its stability and performance. In addition, the interval widths' upper bound is estimated a priori. Finally, two numerical simulations are conducted to test the performance of the designed method. It is concluded that the proposed interval estimator generates more accurate boundaries and performs better. However, the proposed technique can currently be applied in linear and nonlinear discrete-time models. The interval estimator design approach for continuous-time systems will be investigated in the future.

Author Contributions: Conceptualization, A.K.; methodology, A.K.; software, A.K.; validation, A.K., X.B.; formal analysis, A.K., B.Z.; investigation, A.K., B.Z., P.Y.; writing—original draft preparation, A.K., X.B. and M.I.; writing—review and editing, A.K., A.R. and W.X.; supervision, B.Z. All authors have read and agreed to the published version of the manuscript.

Funding: This work was supported in part by the National Natural Science Foundation of China (NSFC) under the grant 62173234 and 62003217.

Institutional Review Board Statement: Not applicable.

Informed Consent Statement: Not applicable.

Data Availability Statement: Not applicable.

Conflicts of Interest: The authors declare no conflict of interest.

References

1. World Health Organization (WHO). *HIV/AIDS*; Global Health Observatory (GHO) Data; WHO: Geneva, Switzerland, 2020. Available online: https://www.who.int/data/gho/data/themes/hiv-aids (accessed on 6 April 2022).
2. World Health Organization. *Seasonal Influenza*; Global Health Observatory (GHO) Data; WHO: Geneva, Switzerland, 2020. Available online: https://www.who.int/news-room/fact-sheets/detail/influenza-(seasonal) (accessed on 6 April 2022).

3. Dukic, V.; Lopes, H.F.; Polson, N.G. Tracking epidemics with Google flu trends data and a state-space SEIR model. *J. Am. Stat. Assoc.* **2012**, *107*, 1410–1426. [CrossRef]
4. Fallas-Monge, J.J.; Chavarria-Molina, J.; Alpizar-Brenes, G. Combinatorial metaheuristics applied to infectious disease models. In Proceedings of the 2016 IEEE 36th Central American and Panama Convention (CONCAPAN XXXVI), San Jose, Costa Rica, 9–11 November 2016; pp. 1–6.
5. Grassly, N.C.; Fraser, C. Mathematical models of infectious disease transmission. *Nat. Rev. Microbiol.* **2008**, *6*, 477–487. [CrossRef] [PubMed]
6. Kaplan, E.H.; Craft, D.L.; Wein, L.M. Emergency response to a smallpox attack: The case for mass vaccination. *Proc. Natl. Acad. Sci. USA* **2002**, *99*, 10935–10940. [CrossRef] [PubMed]
7. Keeling, M.J.; Rohani, P. *Modeling Infectious Diseases in Humans and Animals*; Princeton University Press: Princeton, NJ, USA, 2011.
8. Kermack, W.O.; McKendrick, A.G. A contribution to the mathematical theory of epidemics. *Proc. R. Soc. Lond. Ser. A Contain. Pap. A Math. Phys. Character* **1927**, *115*, 700–772.
9. Feng, Z.; Huang, W.; Castillo-Chavez, C. On the role of variable latent periods in mathematical models for tuberculosis. *J. Dyn. Differ. Equs.* **2001**, *13*, 425–452. [CrossRef]
10. Castillo-Chavez, C.; Cooke, K.; Huang, W.; Levin, S.A. On the role of long incubation periods in the dynamics of acquired immunodeficiency syndrome (AIDS). *J. Math. Biol.* **1989**, *27*, 373–398. [CrossRef]
11. Hethcote, H.W. The mathematics of infectious diseases. *SIAM Rev.* **2000**, *42*, 599–653. [CrossRef]
12. Alonso-Quesada, S.; la Sen, M.D.; Agarwal, R.; Ibeas, A. An observer-based vaccination control law for an SEIR epidemic model based on feedback linearization techniques for nonlinear systems. *Adv. Differ. Equs.* **2012**, *161*, 1–32. [CrossRef]
13. Alonso-Quesada, S.; la Sen, M.D.; Ibeas, A. On the discretization and control of an SEIR epidemic model with a periodic impulsive vaccination. *Commun. Nonlinear Sci. Numer. Simul.* **2017**, *42*, 247–274. [CrossRef]
14. Degue, K.H.; Efimov, D.; Iggidr, A. Interval estimation of sequestered infected erythrocytes in malaria patients. In Proceedings of the 2016 European Control Conference (ECC), Aalborg, Denmark, 29 June–1 July 2016; pp. 1141–1145.
15. Efimov, D.; Perruquetti, W.; Raissi, T.; Zolghadri, A. On interval observer design for time-invariant discrete-time systems. In Proceedings of the 2013 European Control Conference (ECC), Zurich, Switzerland, 17–19 July 2013; pp. 2651–2656.
16. Efimov, D.; Polyakov, A.; Fridman, E.; Perruquetti, W.; Richard, J.-P. Delay-dependent positivity: Application to interval observers. In Proceedings of the 2015 European Control Conference (ECC), Linz, Austria, 15–17 July 2015; pp. 2074–2078.
17. Efimov, D.; Raissi, T.; Zolghadri, A. Control of nonlinear and LPV systems: Interval observer-based framework. *IEEE Trans. Autom. Control* **2013**, *58*, 773–778. [CrossRef]
18. Gouze, J.-L.; Rapaport, A.; Hadj-Sadok, M.Z. Interval observers for uncertain biological systems. *Ecol. Model.* **2000**, *133*, 45–56. [CrossRef]
19. Gucik-Derigny, D.; Raissi, T.; Zolghadri, A. A note on interval observer design for unknown input estimation. *Int. J. Control* **2016**, *89*, 25–37. [CrossRef]
20. Mazenc, F.; Dinh, T.N.; Niculescu, S.I. Interval observers for discrete-time systems. *Int. J. Robust Nonlinear Control* **2014**, *24*, 2867–2890. [CrossRef]
21. Khan, A.; Xie, W.; Zhang, L.; Liu, L.-W. Design and applications of interval observers for uncertain dynamical systems. *IET Circuits Devices Syst.* **2020**, *14*, 721–740. [CrossRef]
22. Khan, A.; Xie, W.; Bo, Z.; Liu, L.-W. A survey of interval observers design methods and implementation for uncertain systems. *J. Frankl. Inst.* **2021**, *358*, 3077–3126. [CrossRef]
23. Degue, K.H.; Efimov, D.; Richard, J.-P. Stabilization of linear impulsive systems under dwell-time constraints: Interval observer-based framework. *Eur. J. Control.* **2018**, *42*, 1–14. [CrossRef]
24. Moisan, M.; Bernard, O. Interval observers for non monotone systems. Application to bioprocess models. In Proceedings of the IFAC Proceedings Volumes, Puebla, Mexico, 14–25 November 2005; Volume 38, pp. 43–48.
25. Rotondo, D.; Cristofaro, A.; Johansen, T.A.; Nejjari, F.; Puig, V. State estimation and decoupling of unknown inputs in uncertain LPV systems using interval observers. *Int. J. Control* **2018**, *91*, 1944–1961. [CrossRef]
26. Yousfi, B.; Raissi, T.; Amairi, M.; Gucik-Derigny, D.; Aoun, M. Robust state estimation for singularly perturbed systems. *Int. J. Control* **2017**, *90*, 566–579. [CrossRef]
27. Degue, K.H.; Ny, J.L. Estimation and outbreak detection with interval observers for uncertain discrete-time SEIR epidemic models. *Int. J. Control* **2020**, *93*, 2707–2718. [CrossRef]
28. Degue, K.H.; Ny, J.L. An interval observer for discrete-time SEIR epidemic models. In Proceedings of the 2018 Annual American Control Conference (ACC), Milwaukee, WI, USA, 27–29 June 2018; pp. 5934–5939.
29. Efimov, D.; Raissi, T. Design of interval observers for uncertain dynamical systems. *Autom. Remote Control* **2016**, *77*, 191–225. [CrossRef]
30. Mazenc, F.; Bernard, O. Asymptotically stable interval observers for planar systems with complex poles. *IEEE Trans. Autom. Control* **2009**, *55*, 523–527. [CrossRef]
31. Mazenc, F.; Bernard, O. Interval observers for linear time-invariant systems with disturbances. *Automatica* **2011**, *47*, 140–147. [CrossRef]
32. Diaby, M.; Iggidr, A.; Sy, M. Observer design for a schistosomiasis model. *Math. Biosci.* **2015**, *269*, 17–29. [CrossRef] [PubMed]

33. Robinson, E.I.; Marzat, J.; Raissi, T. Interval observer design for unknown input estimation of linear time-invariant discrete-time systems. *IFAC-PapersOnLine* **2017**, *50*, 4021–4026. [CrossRef]
34. Efimov, D.; Raissi, T.; Chebotarev, S.; Zolghadri, A. Interval state observer for nonlinear time varying systems. *Automatica* **2013**, *49*, 200–205. [CrossRef]
35. Chebotarev, S.; Efimov, D.; Raissi, T.; Zolghadri, A. Interval observers for continuous-time LPV systems with L1/L2 performance. *Automatica* **2015**, *58*, 82–89. [CrossRef]
36. Guo, S.; Zhu, F. Interval observer design for discrete-time switched system. *IFAC-PapersOnLine* **2017**, *50*, 5073–5078. [CrossRef]
37. Khan, A.; Xie, W.; Zhang, L. Interval state estimation for linear time-varying (LTV) discrete-time systems subject to component faults and uncertainties. *Arch. Control Sci.* **2019**, *29*, 289–305.
38. Liu, L.-W.; Xie, W.; Khan, A.; Zhang, L.-W. Finite-time functional interval observer for linear systems with uncertainties. *IET Control Theory Appl.* **2020**, *14*, 2868–2878. [CrossRef]
39. Yi, Z.; Xie, W.; Khan, A.; Xu, B. Fault detection and diagnosis for a class of linear time-varying (LTV) discrete-time uncertain systems using interval observers. In Proceedings of the 2020 39th Chinese Control Conference (CCC), Shenyang, China, 27–29 July 2020; pp. 4124–4128.
40. Bliman, P.-A.; Barros, B.D.A. Interval observers for SIR epidemic models subject to uncertain seasonality. In Proceedings of the International Symposium on Positive Systems, Fukuoka, Japan, 4–5 November 2016; pp. 31–39.
41. Hu, Z.; Teng, Z.; Jiang, H. Stability analysis in a class of discrete SIRS epidemic models. *Nonlinear Anal. Real World Appl.* **2012**, *13*, 2017–2033. [CrossRef]
42. Mickens, R.E. Numerical integration of population models satisfying conservation laws: NSFD methods. *J. Biol. Dyn.* **2007**, *1*, 427–436. [CrossRef] [PubMed]
43. Bichara, D.; Cozic, N.; Iggidr, A. On the estimation of sequestered infected erythrocytes in Plasmodium falciparum malaria patients. *Math. Biosci. Eng.* **2014**, *11*, 741–759. [CrossRef]
44. Hooker, G.; Ellner, S.P.; Roditi, L.D.V.; Earn, D.J. Parameterizing state–space models for infectious disease dynamics by generalized profiling: Measles in Ontario. *J. R. Soc. Interface* **2011**, *8*, 961–974. [CrossRef] [PubMed]
45. Moore, R.E. *Interval Analysis*; Prentice-Hall: Hoboken, NJ, USA, 1966.
46. Ibeas, A.; Sen, M.D.; Alonso-Quesada, S.; Zamani, I. Stability analysis and observer design for discrete-time SEIR epidemic models. *Adv. Differ. Equs.* **2015**, *2015*, 122. [CrossRef]
47. Rachah, A. Analysis, simulation and optimal control of a SEIR model for Ebola virus with demographic effects. *Commun. Fac. Sci. Univ. Ank. Ser. A1 Math. Stat.* **2018**, *67*, 179–197.